SOURCES OF IRON FOR PYRITE FORMATION IN MARINE SEDIMENTS

ROBERT RAISWELL* and DONALD E. CANFIELD**

ABSTRACT. More than two hundred aerobic continental margin, aerobic deep sea, dysaerobic, and anaerobic/euxinic sediments have been examined for their variations in different operationally defined iron fractions, each of which represents a different reactivity toward dissolved sulfide. Aerobic continental margin, deep sea, and dysaerobic sediments contain similar contents of highly reactive iron (dithionite-soluble iron plus pyrite iron), poorly reactive iron (iron soluble in HCl less that soluble in dithionite), and unreactive iron (total iron less that soluble in HCl). By contrast non-turbidite euxinic samples from the Black Sea, as well as euxinic samples from the Cariaco Basin and Framvaren are enriched in highly reactive iron. These sediments contain a small lithogenous fraction and a large biogenous, organic C-rich fraction, which decays by sulfate reduction in an iron-rich water column to form pyrite-rich sediment. Other anaerobic/euxinic samples from the Black Sea, Orca Basin, and Kau Bay contain lower concentrations of biogenous sediment and are not therefore enriched in highly reactive iron. Degrees of Pyritization (DOP) for all the aerobic, dysaerobic, and anaerobic/euxinic samples (except those low in biogenous material) are consistent with analogous ancient sediments and indicate that most pyrite formation occurs from the highly reactive iron fraction.

INTRODUCTION

Pyrite is formed in anoxic marine sediments by the reaction of dissolved sulfide, produced by microbial sulfate reduction, with detrital iron-bearing minerals (Berner 1970, 1984). The initial products are often iron sulfide minerals which are probably transformed to pyrite by reaction with dissolved sulfide (Rickard, 1997; Rickard and Luther, 1997) and/or polysulfides (Goldhaber and Kaplan, 1974; Rickard, 1975; Luther 1991; Schoonen and Barnes, 1991). Although there are a variety of transformation pathways, the extent of pyrite formation is thought to be limited either by the microbial production of sulfide or by the availability of reactive iron minerals (Canfield and Raiswell, 1991).

The availability of reactive iron minerals probably limits pyrite formation in many of the most commonly-studied sedimentary environments, notably continental margin sediments, and as a result there is considerable interest in defining the reactivity of iron minerals toward dissolved sulfide. Berner (1970) used a boiling HCl extraction for one minute to estimate the maximum iron available for reaction. This extraction removes iron from iron oxides and also extracts significant amounts of iron from iron-bearing chlorites and smectites (Raiswell, Canfield, and Berner, 1994). However Canfield (ms) and Canfield, Raiswell, and Bottrell (1992) point out that many continental margin sediments still contain iron which can be extracted by boiling HCl, even though the persistence of dissolved sulfide in the porewaters indicates only slow removal by precipitation with iron. It follows that at least part of the iron extracted by the boiling HCl technique must be only poorly reactive toward dissolved sulfide.

The modern sediment studies of Canfield (ms and 1989) also provide further crucial observations by showing that the abundance of iron oxides essentially controls the presence of dissolved sulfide in sediment porewaters. Thus the iron oxides (ferrihydrite, goethite, haematite, and lepidocrocite) react rapidly with dissolved sulfide, and, as long as these minerals are present, dissolved sulfide is absent from the porewaters. Once the iron oxides are consumed, the residual iron minerals react only slowly with dissolved sulfide which is therefore able to accumulate in the porewaters.

* Department of Earth Sciences, Leeds University, Leeds LS2 9JT, United Kingdom
** Institute of Biology, Odense University, Campusvej 55, 5230 Odense M, Denmark

These observations have lead Canfield, Raiswell, and Bottrell (1992) to define the reactivities of iron minerals by estimating their half-lives with respect to sulfidation (table 1). The data show that there are effectively two main pools of sediment iron (see also Morse and Wang, 1997): one comprises the iron oxides which react rapidly with dissolved sulfide (with half-lives of less than 1 month), and the other comprises iron-bearing silicates which react much more slowly (with half-lives of at least 80,000 yrs). A recent and more detailed study of Peru Margin sediments (Raiswell and Canfield, 1996) shows that some iron silicate phases that are soluble in boiling HCl may react extremely slowly, exhibiting half-lives of several million years with respect to reaction with dissolved sulfide. In these circumstances only small proportions of the iron silicates may be pyritized. Thus, the near-surface HCl-soluble silicate iron content of the Peru Margin sediments is 0.8 to 1.0 percent Fe, but only 30 to 60 percent of this Fe is pyritized despite exposure to dissolved sulfide for several million years.

These data suggest that the maximum abundance of pyrite (given the presence of sufficient metabolizable organic matter) is substantially controlled by the burial flux of iron oxides into a sediment (but see also Morse and Berner, 1995), and is only increased to a limited extent (depending on sedimentation rate) by the subsequent exposure of HCl-soluble silicate iron to dissolved sulfide. However this conclusion appears to conflict with observations on the Degree of Pyritization (DOP) values in ancient sediments, where DOP is defined as;

$$DOP = \text{Pyrite Fe}/(\text{Pyrite Fe} + \text{HCl-soluble Fe}).$$

Raiswell and others (1988) have shown that ancient laminated, organic carbon-rich sediments, deposited beneath essentially anoxic or sulfidic bottom waters, have DOP values which range from 0.75 to 1.0 (see also Leventhal and Hosterman, 1982). These DOP values appear to indicate that HCl-soluble Fe can, in some circumstances, be almost entirely pyritized.

Such differences between modern and ancient sediments could arise if burial recrystallization of Fe-bearing silicates caused less Fe to be soluble in HCl (Middelburg, personal communication); however, recent work on the Black Sea (Canfield, Lyons, and Raiswell, 1996) suggests a different way of resolving this conflict. Thus the Black Sea shows seasonal and/or spatial variations in the deposition of biogenous and lithogenous debris. The decomposition of settling, organic matter-rich, biogenous particles by sulfate reduction generates hydrogen sulfide in the upper, dissolved Fe-rich and oxygen-depleted part of the water column. Here iron sulfides form using the water column dissolved Fe derived from the reductive dissolution of oxide phases. Thus, associated with a high depositional flux of biogenous debris is a high depositional flux of Fe sulfides producing high DOP values of up to 0.8 in the sediments. Conversely, when the flux of

TABLE 1

Rate constants and half-lives of sedimentary iron minerals with respect to their reaction with dissolved sulphide (from Canfield, Raiswell, and Bottrell, 1992)

Iron Mineral	Rate Constant (yr^{-1})	Half-life
Ferrihydrite	2 200	2.8 hr
Lepidocrocite	>85	<3 days
Goethite	22	11.5 days
Haematite	12	31 days
Magnetite (uncoated)	6.6×10^{-3}	105 years
'Reactive' silicates	3.0×10^{-3}	230 years
Sheet silicates	8.2×10^{-6}	84 000 years
Ilmenite, garnet, augite, amphibole	$\ll 8.2 \times 10^{-6}$	$\gg$84 000 years

lithogenous debris is high, the low amount of reactive iron associated with these particles produces low DOP values of 0.3 to 0.5, typical of sulfidic normal marine sediments.

The Black Sea data indicate that high DOP values may arise in anaerobic/euxinic environments because of the water-column formation of Fe sulfides associated with the anaerobic decomposition of settling biogenous debris. High DOP values do not necessarily arise because of high concentrations of dissolved sulfide and/or long contact times between dissolved sulfide and sedimentary Fe-bearing lithogenous particles. Support for this view is also provided by the Peru Margin data discussed above, which implies that the HCl-soluble iron in silicates (an important component of the lithogenous fraction) is only very slowly pyritized even with prolonged exposure to dissolved sulfide.

It is the purpose of this paper to determine the contributions of highly reactive iron (as iron oxides) and poorly reactive iron (extracted from silicates by boiling HCl) to sediments from a range of different depositional environments including aerobic (continental margin and deep sea), dysaerobic, and anaerobic/euxinic sediments. These data will be used to demonstrate the mineralogical controls on DOP. Further, these data provide the first comprehensive survey of Fe speciation in marine sediments, which will be used to establish whether Black Sea-type processes of reactive iron enrichment also occur in other modern anaerobic/euxinic depositional environments, and whether the magnitude of any such enrichment depends on the degree of bottom water oxygenation.

SAMPLE DESCRIPTION AND CLASSIFICATION

Samples for this study were either obtained from our own libraries of sediment material, donated by other researchers of modern sediments, or were selected from various core libraries (for example Lamont-Doherty). Depositional environments were classified according to bottom water oxygenation levels, with a further sub-division according to water depth as explained below. This strategy was adopted to explore for possible relationships between Fe speciation and bottom water oxygen levels, as well as any possible controls of Fe speciation by proximity to land.

Aerobic.–Bottom water oxygen concentrations in excess of 80 micromolar: These concentrations roughly correspond to the aerobic category of Tyson and Pearson (1991; see also Wignall, 1994), which has oxygen concentrations in excess of 2 ml l^{-1}. This value is somewhat larger than that proposed by Rhoads and Morse (1971) and Rhoads and others (1991), however the lower values are still apparently sufficient to support an active calcareous benthic fauna. Aerobic samples are further sub-divided by water depth into Continental Margin (less than 1000 m) and Deep Sea (more than 1000 m depth). A water depth of 1000 m is chosen as approximating the edge of the continental shelf, separating the continental margin from the deep-sea.

Dysaerobic.–Bottom water oxygen concentrations from 5 to 80 micromolar, again roughly corresponding to the classification of Tyson and Pearson (1991), which covers concentrations from 0.1 to 2 ml l^{-1}: Savrda, Bottjer, and Gorsline (1984) point out that there is no sharp faunal change between the dysaerobic and aerobic categories, but oxygen levels below 0.3 ml l^{-1} (or 13 micromolar) are usually associated with weak benthic activity and the formation of laminated sediments (Wignall, 1994; but see also Savrda, Bottjer, and Gorsline, 1984).

Anaerobic/Euxinic.–Bottom water oxygen concentrations below 5 micromolar or dissolved sulfide present: This oxygen level corresponds to the boundary adopted by Tyson and Pearson (1991), and Rhoads and Morse (1971). All the samples in this category were chosen to have bottom waters which are sufficiently oxygen-depleted either to contain dissolved iron or dissolved sulfide, although only a limited range of modern environments satisfy this criteria (see below).

Sample sites are described briefly in app. 1, 2, 3, and 4. Each site is generally represented by no more than 2 samples; one near-surface sample (usually within the top 30 cm) and one deeper sample (usually from 50–100 cm below the sediment surface). The choice of depths was often pre-determined by sample availability. The Continental Margin Aerobic sample sites are summarized in app. 1 and comprise 24 different cores (46 samples) ranging in water depth from 1.5 to 760 m and in sedimentation rate from 0.07 to 2.0 cm yr^{-1}. Deep Sea Aerobic samples are listed in app. 2. This data set contains 36 different cores (56 samples) with water depths from 1015 to 5592 m and sedimentation rates from 0.07 to 1.4×10^{-4} cm yr^{-1}. The majority of these samples are from the Lamont-Doherty Core Library and represent foraminiferal marls of varying carbonate content ($CaCO_3$ ranges from 2–90 percent). The Dysaerobic samples (app. 3) are collected from 14 cores and comprise 26 samples with sedimentation rates ranging from 0.4 to 0.001 cm yr^{-1}.

There are relatively few modern environments that fall into the category of Anaerobic/Euxinic, and we have obtained 41 samples from a majority of the environments that have been explored, including the Black Sea, Cariaco Basin, Framvaren, Kau Bay, and the Orca Basin. All these samples have been used in our data base. We have additionally used literature data from a further 50 Black Sea samples. To compare these data we will pay attention to basinal properties, such as water depth, sedimentation rate, and proximity to land masses.

To summarize, Framvaren and Kau Bay (deep basin) are both relatively small (approx 10 km^2 and 800 km^2, respectively) and shallow (160 m for Framvaren and 500 m for Kau Bay) and are entirely surrounded by land. Sedimentation rates in Framvaren are slow at about 0.01 cm yr^{-1} (Skei, 1983). Further, Framvaren has a well established anoxic zone with high concentrations of dissolved sulfide and an overlying suboxic zone with dissolved Fe^{2+} of up to 800 nM (Saelen and others, 1993). Kau Bay is intermittantly euxinic and dysaerobic' and has variable sedimentation rates of 0.07–1.0 cm yr^{-1} (Middelburg, ms and 1991). Water column dissolved Fe^{2+} concentrations have not been reported. By contrast, the Black Sea, while land-locked, is quite large (500,000 km^2), with a deep basin of approx 2000 m water depth and microlaminated sediments depositing at a rather slow sedimentation rate of between 0.013 to 0.02 cm yr^{-1} (Arthur and others, 1994; Crusius and Andersen, 1991). Dissolved Fe^{2+} reaches levels of up to 1000 nM at the oxic/anoxic interface (Brewer and Spencer, 1974). The Cariaco Basin is also rather large (10,000 km^2) and deep (max 1400 m approx) but occurs within a continental shelf environment. Consequently, sediments deposit more rapidly, at between 0.06 to 0.1 cm yr^{-1}, than in deep basin areas of the Black Sea (Lyons and others, 1996). Dissolved Fe^{2+} concentrations just below the oxic/anoxic interface of up to around 500 nM have been reported (Bacon and others, 1980). The Orca Basin is relatively small (400 km^2) and is located on the continental shelf in the Gulf of Mexico. Dissolution of near-by salt diapirs has generated a dense brine in the bottom-waters of the basin. This brine limits the exchange of deep basinal waters, resulting in oxygen depletion in these waters. Sedimentation rates are around 0.1 cm yr^{-1}, and dissolved Fe^{2+} in the brine pool reaches almost 0.03 mM, with dissolved sulfide less than 1 micromolar (Trefry and others, 1984; Sheu and Presley, 1986).

ANALYTICAL METHODS AND THEIR CROSS-CALIBRATION

Analytical methodology.–Sediments were collected by a variety of techniques (details of which can be found in the references cited for each locality) and are accordingly subject to different types of error that affect measurement of the different iron species and total or sulfide sulfur, see below.

Total iron was measured either by XRF or by the wet chemical method of Aller, Mackin, and Cox (1986) which involved 12 hrs heating of the sample in a muffle furnace, with the iron then leached with hot 12 M HCl. After the leaching period, solutions were diluted and measured by atomic absorption, using standards of a similar HCl concentration. This wet chemical method has been calibrated against XRF measurements on 30 different modern sediments with a range from 1 to 6 percent total Fe (see Raiswell and Canfield, 1996). The data gave a regression line of;

$$(Fe_{XRF}) = 0.997 \, (Fe_{WET}) + 0.016 \qquad r = 0.98.$$

The precision of the wet chemical method was measured as 3 percent.

Iron extractions were carried out using the dithionite method of Canfield (1989) and the boiling HCl method of Berner (1970). These iron extractions have been examined by Canfield (ms) and Raiswell, Canfield, and Berner (1994), who concluded that dithionite quantitatively extracts the iron oxide/oxyhydroxide phases (lepidocrocite, ferrihydrite, goethite, and haematite) with only relatively small amounts extracted from iron silicates. The boiling HCl method also quantitatively extracts the same oxides but, in addition, removes several percent more iron from silicate phases (see table 2 in Raiswell, Canfield, and Berner, 1994). Precisions of 3 to 4 percent for the dithionite extraction and 5 percent for the boiling HCl extraction were estimated by Raiswell, Canfield, and Berner (1994). Note that dithionite and boiling HCl also dissolve AVS, but pyrite is insoluble in both treatments (Canfield, 1989; Berner, 1970).

These iron analyses can be used (Raiswell and Canfield, 1996) to recognize different, operationally-defined, sediment iron pools. The iron extracted by dithionite (FeD) from oxides (and the small amount removed from silicates) is considered to be highly reactive toward dissolved sulfide (Canfield, Raiswell, and Bottrell, 1992). Prior to diagenesis the initial highly-reactive pool would therefore comprise FeD and all the Fe now present as pyrite and AVS (FeP) together expressed as Fe_{HR}. The boiling HCl technique removes iron (FeH) extracted by dithionite (oxides plus some from silicates) together with additional iron from a wide range of silicates. Raiswell and Canfield (1996) have shown that this additional Fe extracted from silicates is sulfidized only on a million year time scale, hence FeH-FeD represents an iron fraction which reacts only slowly with dissolved sulfide and is here termed poorly-reactive or Fe_{PR}. Finally, the total iron content (FeT) can be used to define the remaining fraction of iron, mainly in silicates, which is essentially unreactive (Fe_U);

$$Fe_U = FeT - (FeP + FeD) - (FeH - FeD) = FeT - FeP - FeH$$

Our convention is that subscripts (for example Fe_{HR}) indicate an operationally defined iron fraction, whereas analytical values are denoted by capital letters (for example FeT).

Our analytical procedures were as follows. All samples were air-dried (if received wet) and disaggregated by hand with an agate pestle and mortar. With a large number of samples we initially chose to estimate FeP from gas chromatography elemental analyzer measurements of total S, however errors then arose from: (1) The presence of porewater sulfate. In no case was porewater sulfate washed free from the samples so, for all samples except those experiencing complete sulfate depletion due to sulfate reduction, some sulfate will contribute to total sulfur analyses. This is in addition to the sulfur present as solid phase sulfides. (2) Oxidation effects. Samples had often been air-dried by storage under different conditions for variable lengths of time. Partial oxidation of acid volatile sulfides (and pyrite) has probably occurred in most cases. However oxidation of pyrite does not necessarily result in low total sulfur values (if the oxidized sulfur is retained in the sediment; see Canfield and others, 1986), but does produce dithionite-soluble Fe. In these circumstances pyrite oxidation products contribute to measurements of both total S and FeD and may over-estimate Fe_{HR}.

Errors arising from (1) can be avoided by measuring pyrite sulfur directly by wet chemical methods. Errors arising from (2) will then produce low values for pyrite sulfur, but this artifact does not present a problem in the present context, because the iron oxide phases produced by sulfide oxidation are extractable by dithionite (Raiswell, Canfield, and Berner, 1994), and the main aim of the present work is to measure a highly reactive iron fraction which is actually defined (see above) as the sum of pyritic iron plus dithionite extractable iron.

We have therefore chosen to measure pyrite sulfur directly on all samples where total S exceeds 0.5 percent (which includes some continental margin samples and all dysaerobic and anaerobic/euxinic samples), since oxidation effects on these sulfide-rich samples could potentially produce large errors in Fe_{HR}. These samples were analyzed for total reducible sulfur (TRS) by chromous chloride reduction using the method of Canfield and others (1986), as modified by Newton and others (1995). All TRS was assumed to be pyrite. Samples with total S less than 0.5 percent (all deep sea and some continental margin samples) were analyzed for total S by gas chromatography (using a Carlo Erba 1500 Elemental Analyser). Total sulfur values on these samples were corrected for porewater sulfate, mainly using literature data for porosity and porewater sulfate, and the remaining sulfur was assumed to be pyritic.

Using this approach, figure 1A shows the correlation between pyrite S and total S (corrected for seawater sulfate) for 47 aerobic and dysaerobic samples. Some variability is apparent (due to oxidation effects, the loss of porewater sulfate during the storage of highly porous samples, and the presence of non-sulfidic sulfur) but the regression line indicates a close relationship between pyrite and total sulfur;

$$\text{Total S} = 1.02 \text{ (Pyrite S)} \qquad r = 0.89$$

Additional anaerobic/euxinic data sets.–We had particular difficulty in obtaining a large and representative set of sediments from anaerobic/euxinic sites for analysis. There are, however, various sets of Fe-speciation data in the literature from such sediments, particularly for the Black Sea, that can be cross-calibrated to match our own Fe extraction procedures and operational Fe-pool definitions. Hence we have sought to combine literature Black Sea iron data from Rozanov, Volkov, and Yagodinskaya (1974), Calvert and Karlin (1991), and Lyons (ms) by converting all the data, as best possible, to the operationally defined Fe pools described above.
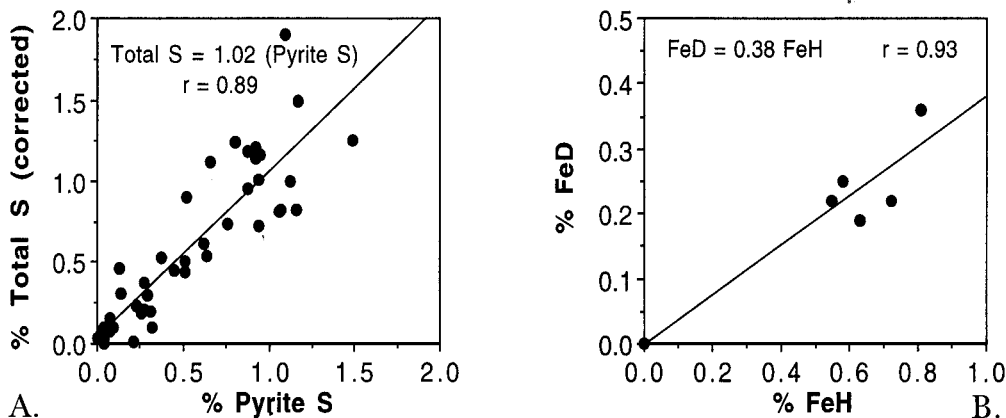

Fig. 1(A) Relation of total sulfur (corrected for the presence of porewater sulfate) to pyrite sulfur for aerobic and dysaerobic samples. (B) Relation of dithionite-extractable iron to HCl-extractable iron in Black Sea sediments.

We use the Black Sea data of Rozanov, Volkov, and Yagodinskaya (1974) for samples from H_2S-bearing bottom waters at depths greater than 500 m. These are surface grab samples of the upper few cms of sediment and probably comprise both laminated Unit I sediments and turbidites that are sporadically emplaced over the bottom of the deep basin (Lyons, ms; Canfield, Lyons, and Raiswell, 1996). Exact details of the iron extraction procedures are not given; however Rozanov, Volkov, and Yagodinskaya (1974) assign iron to the following species; Fe^{3+} (HCl-soluble), Fe^{2+} (HCl-soluble), Fe as monosulfide and Fe as pyrite. We assume that Fe^{3+} represents iron oxides and will be roughly equivalent to our FeD, that Fe^{2+} is roughly equivalent to our FeH − FeD (Fe_{PR}), and that the sum of monosulfide and pyritic iron is equivalent to FeP. Rozanov, Volkov, and Yagodinskaya (1974) also give the carbonate contents of their samples.

Calvert and Karlin (1991) have data for laminated, deep basin sediments in H_2S-bearing bottom waters (stations 9 and 14 of the 1988 Black Sea expedition) which show the iron present as FeH, FeP, and FeT. To provide an estimate of FeD from this data set, we have cross-calibrated a Black Sea core made available to us by Lyons (personal communication) and analyzed using the methods described above. An estimate of FeD was therefore obtained from the correlation of FeD with FeH (fig. 1B) in our own Black Sea core. Calvert (personal communication) has also supplied $CaCO_3$ data for his cores from stations 9 and 14, although these are usually from depths close (but not identical) to the sample data published. We have estimated $CaCO_3$ contents by extrapolation between adjacent depths.

Lyons (ms) has analyzed the laminated, deep basin sediments at the same stations 9 and 14 and reports the iron present as FeH, FeT, and FeP. There is also a measurement of the iron extracted by hydroxylamine hydrochloride in 25 percent acetic acid. Measurements of the iron extracted by this methodology on our own Black Sea core (0.03–0.29 percent) are on average about 50 percent lower than the iron extracted by dithionite (0.19–0.42 percent), although there was only an erratic relationship between the two iron determinations (presumably due to relatively large analytical errors at these concentration levels). However Aller, Mackin, and Cox (1986) and Wallman and others (1993) confirm that the hydroxylamine extraction dissolves considerably less iron than the dithionite extraction, and we have therefore estimated FeD by multiplying the iron extracted by hydroxylamine by 1.5. An estimate of FeD can also be made using figure 1B and the FeH data of Lyons (ms), and these FeD values are all (except one) within 0.05 wt percent of those based on the corrected values of the hydroxylamine extraction. These different procedures for estimating FeD appear self-consistent in that comparable ranges of FeD (wt percent) are produced: 0.19 to 0.36 for our own core, 0.10 to 0.15 and 0.10 to 0.24 respectively based on the corrected hydroxylamine and FeH data for the Lyons (ms) samples, 0.06 to 0.43 (Calvert and Karlin, 1991), and 0 to 0.32 (Rozanov, Volkov, and Yagodinskaya (1974). Together all the iron data from these four studies comprise our Black Sea data base.

<center>RESULTS</center>

Fe speciation in aerobic and dysaerobic sediments.—Aerobic and dysaerobic data sets are first considered together, while anaerobic/euxinic data will be considered below. Overall the data represent a comprehensive survey of iron speciation, with the 219 analyses providing good coverage of each depositional environment (although the geographical spread is uneven). Table 2 shows the results from recasting the analytical data into the iron pools defined above. The data are uncorrected for the dilution effects of biogenous carbonate and organic matter, as it is our intention to focus mainly on the ratios of each of the iron pools with total iron, but we note that there are surprisingly few significant differences (on a students "t" test) in the means and standard deviations of the

TABLE 2

Mean and standard deviations of iron species in aerobic and dysaerobic sediments

Depositional Environment	Wt % Fe present as			
	Fe_{HR} (FeD + FeP)	Fe_{PR} (FeH − FeD)	Fe_U (FeT − FeH − FeP)	FeT
Continental Margin	0.82 ± 0.31	0.66 ± 0.28	1.39 ± 0.39	2.92 ± 0.78
Deep Sea	0.71 ± 0.35	0.80 ± 0.59	1.55 ± 0.75	3.08 ± 1.25
Dysaerobic	0.93 ± 0.46	1.06 ± 0.51	1.42 ± 0.64	3.42 ± 1.08

	Ratios of Fe species to total Fe		
	(FeD + FeP)/FeT	(FeH − FeD)/FeT	Fe_U/FeT
Continental Margin	0.28 ± 0.06	0.23 ± 0.07	0.50 ± 0.06
Deep Sea	0.25 ± 0.10	0.26 ± 0.15	0.49 ± 0.15
Dysaerobic	0.28 ± 0.10	0.31 ± 0.09	0.42 ± 0.12

Where Fe_{HR} = Highly reactive iron, Fe_{PR} = Poorly reactive iron, and Fe_U = Unreactive iron.

highly reactive (Fe_{HR}), poorly reactive (Fe_{PR}), and unreactive iron (Fe_U) pools in each depositional environment. The only difference significant at the 0.1 percent level is between the poorly reactive iron contents of the continental margin and dysaerobic samples. The total iron contents are not significantly different at less than the 2 percent level, although their similarities simply reflect similar dilution effects from biogenous material. Overall, table 2 shows that the total iron is comprised of, on average, 25 to 28 percent highly reactive iron, 23 to 31 percent poorly reactive iron, and 42 to 50 percent unreactive iron. There is remarkably little variation in the mean proportions of Fe_{HR} in these different depositional environments.

Figure 2 shows the relationships between the highly reactive iron fraction and total iron for the aerobic (continental margin and deep sea) and dysaerobic samples. All these groups of samples show crude trends of increasing Fe_{HR} with increasing total iron (which only rarely exceeds 5 percent). For comparative purposes, each figure shows upper and lower boundaries at

$$(FeD + FeP) = 0.38 \, FeT \tag{1}$$

$$(FeD + FeP) = 0.06 \, FeT \tag{2}$$

which define the envelope encompassing the continental margin data set. The combined aerobic and dysaerobic data sets fall inside the same envelope (fig. 2). Mean and standard deviations for the ratios of each iron pool to the total iron content (table 2) are consistent with the similarities in figure 2 in that the means and standard deviations of the ratio Fe_{HR}/FeT in continental margin, deep sea, and dysaerobic samples show no significant differences on a students "t" test.

The unreactive iron fraction shows a reasonable linear dependence on total iron in both the aerobic continental margin and deep-sea data sets and a more scattered but still significant relationship for the dysaerobic data set (fig. 3). The means and standard deviations of the ratio Fe_U/FeT in the continental margin (0.50 ± 0.06) and deep sea (0.49 ± 0.15) samples are not significantly different, but both are significantly different from the dysaerobic samples (0.42 ± 0.12) at the 2 percent and <0.1 percent level respectively on a students "t" test. The combined plot of all this data (fig. 3) has a regression line given by;

$$Fe_U = 0.46 \, FeT \qquad r = 0.78 \tag{3}$$
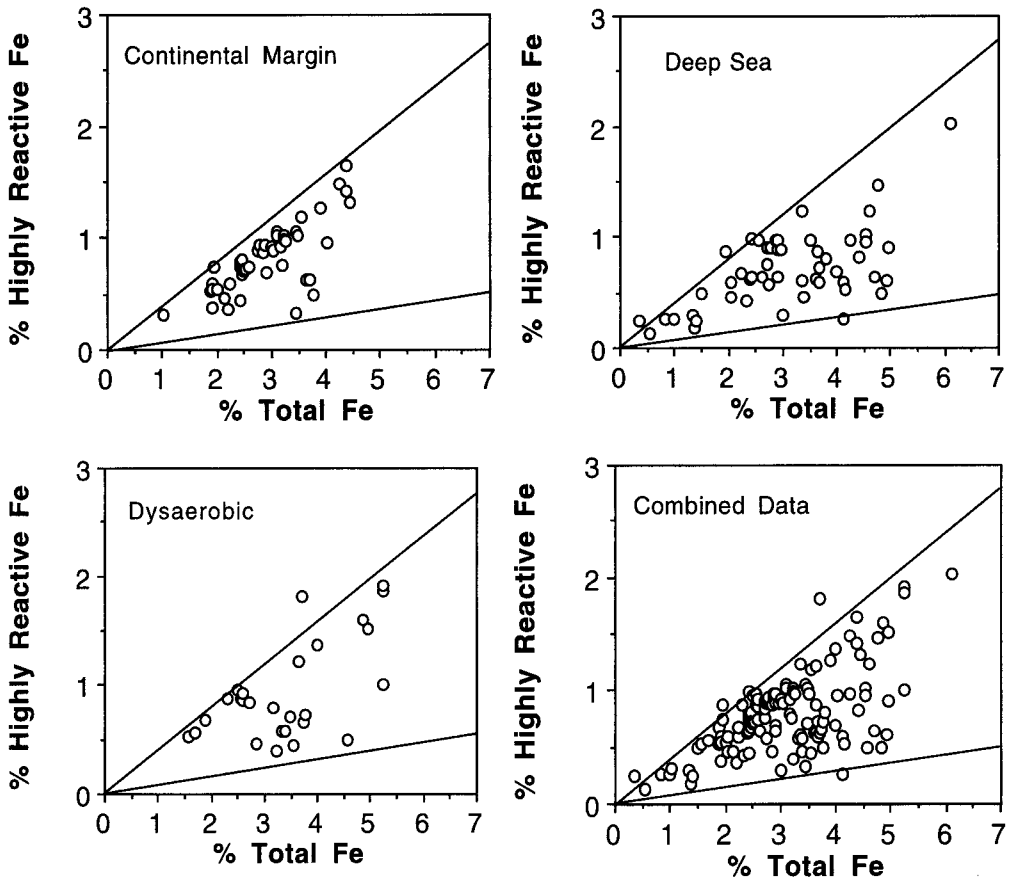
Fig. 2. Variations in the content of highly reactive iron (FeD + FeP) with total iron for continental margin, deep-sea and dysaerobic sediments, and for all data combined. Lines define envelope containing all continental margin data (see text).

indicating that on average about 46 percent of the total iron can be considered as unreactive. A few negative values occur because of the errors arising in estimating small concentrations of Fe_U as the difference between FeT and (FeH + FeP).

The total iron content comprises the sum of three iron fractions (highly reactive, poorly reactive, and unreactive iron) so that the relationships described above between FeT and Fe_{HR} as well as between FeT and Fe_U constrain the relationship between the poorly reactive fraction (Fe_{PR}) and FeT. The means and standard deviations of the ratio Fe_{PR}/FeT in the continental margin (0.23 ± 0.07) and deep sea (0.26 ± 0.15) samples are not significantly different, but the continental margin and dysaerobic (0.31 ± 0.09) samples are significantly different from each other (at the <0.1 percent level) on a students "t" test. The plot of Fe_{PR} against Fe_T for the combined data set is shown in figure 4 with the boundary lines drawn as required for mass balance by substituting eqs (1), (2), and (3) into (4) below;

$$Fe_{PR} = FeT - Fe_U - Fe_{HR} \qquad (4)$$

which gives

$$Fe_{PR} = 0.08 \, FeT$$

and

$$Fe_{PR} = 0.40 \, FeT.$$

Fe speciation in anaerobic/euxinic sediments.—Canfield, Lyons, and Raiswell (1996) have suggested that, within the Black Sea, laminated organic carbon- and carbonate carbon-rich, euxinic sediments receive a high flux of reactive iron compared to carbonate-poor turbidites derived from the basin margins and to aerobically deposited sediments in general (see above). A high flux of reactive iron to basinal Black Sea sediments can be tested by comparing the concentrations of reactive iron in euxinic Black Sea sediments with the aerobic sediments described above. Further, whether this is a general phenomena for anaerobic/euxinic basins can be evaluated from comparisons between the remaining such sites and the aerobic sediment data set. Consistent with previous arguments of Canfield, Lyons, and Raiswell (1996), much of the Black Sea highly reactive iron data (fig. 5) plot significantly above the upper limit given by eq (1) for the combined aerobic data set (fig. 2), demonstrating an enhanced flux of reactive Fe to
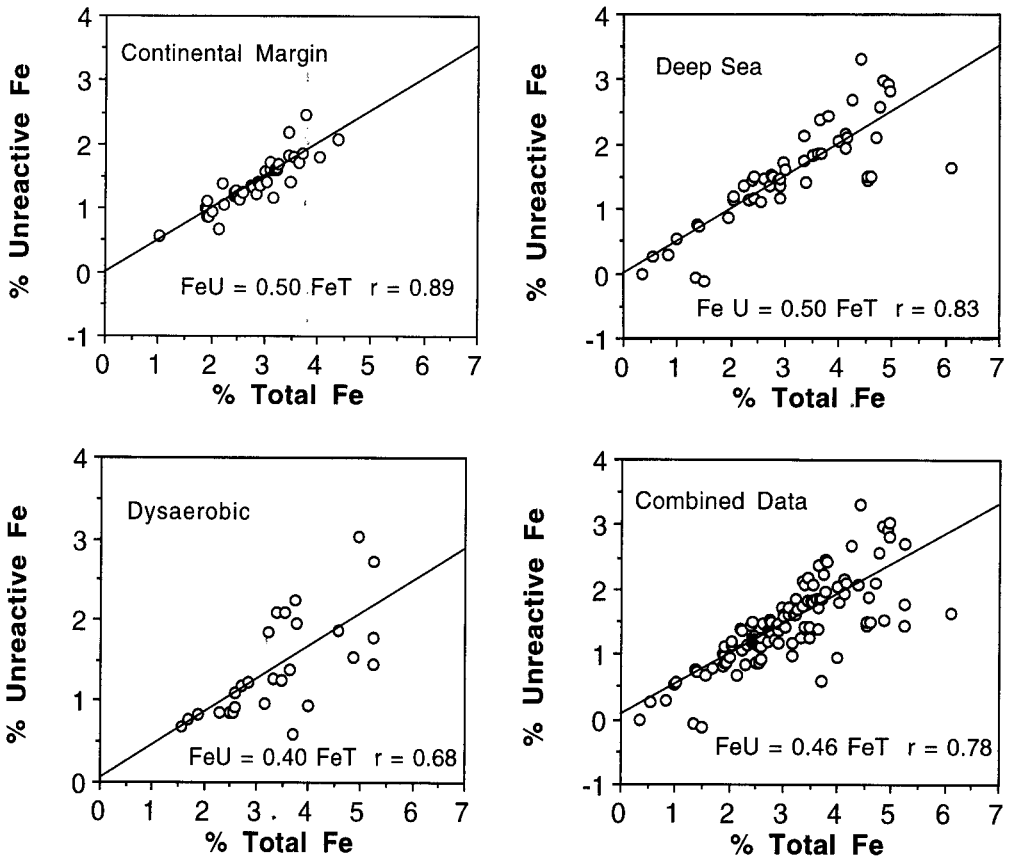

Fig. 3. Variations in the content of unreactive iron (FeT–FeH–FeP) with total iron for continental margin, deep-sea, and dysaerobic sediments and for all data combined.
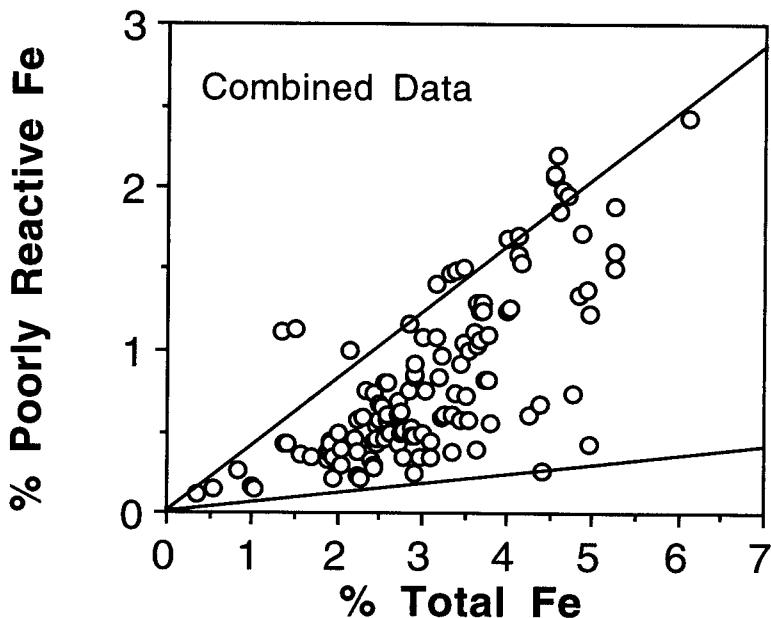
Fig. 4. Variations in the content of poorly reactive iron (FeH–FeD) with total iron for the combined continental margin, deep-sea and dysaerobic data set. Lines define envelope of $Fe_{PR} = 0.08FeT$ and $0.40FeT$ (as required for mass balance, see text).

euxinic Black Sea sediments at a given Total Fe content. The samples that plot below this line (within the aerobic field) are all from Rozanov, Volkov, and Yagodinskaya (1974) which generally have high Fe content, consistent with a predominantly turbidite, or at least lithogenous source. As described by Canfield, Lyons, and Raiswell (1996), such high Fe sediments do not contain the biogenous debris that encourage the sulfidation of reactive Fe within the water-column as described above. Although the results of Rozanov, Volkov, and Yagodinskaya (1974) are generally consistent with our current and previous discussions of reactive iron control in the Black Sea, artifacts for which we have no control (such as potential sulfide oxidation of the samples and loss of oxidized products) could also be of importance in generating the relatively low reactive Fe contents.

Concentrations of Fe_U (fig. 5) show a similar linear trend with FeT as the aerobic samples (see fig. 3), although the regression line in the Black Sea data does not pass through the origin. The scatter of this data and the presence of occasional negative values suggest that analytical errors on the individual measurements have become aggregated during estimation of Fe_U (as the difference between FeT and Fe_{HR}) and are now significant. The slopes of the regression lines for FeU on figures 3 and 5 are similar $(0.46 \pm 0.06$ and $0.56 \pm 0.08)$. The poorly reactive Fe contents (Fe_{PR}) of the Black Sea sediments also fall within the field outlined by the combined aerobic data sets (fig. 5).

The similar overall trends between the poorly reactive (Fe_{PR}) and unreactive (Fe_U) components and FeT in aerobic and euxinic Black Sea sediments suggest that the lithogenous fraction in Black Sea sediments (which contributes to Fe_{PR} and Fe_U) contains Fe of similar reactivity to that found in aerobic sediments deposited around the world.

The Cariaco Basin data provide the same general patterns of behavior as are found in the Black Sea; thus there are analogous enrichments in Fe_{HR} (fig. 6), and the plots of Fe_U against FeT and Fe_{PR} against FeT (fig. 6) both overlap the Black Sea data. These relationships are taken to indicate that the euxinic Cariaco Basin sediments are also enriched in highly reactive iron compared to aerobic sediments.
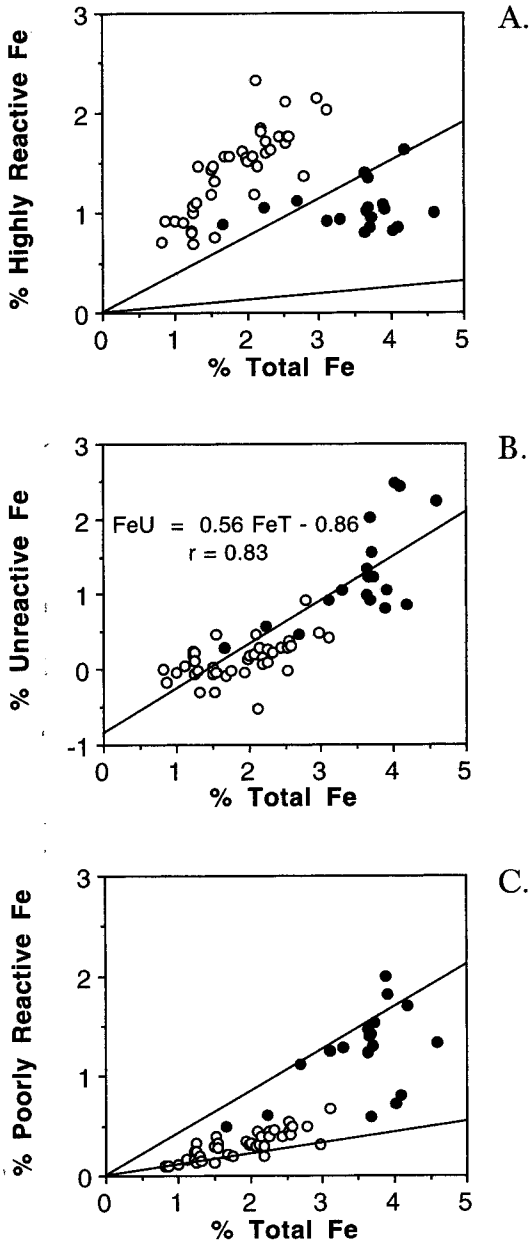
Fig. 5. Variations in the content of (A) highly reactive, (B) unreactive, and (C) poorly reactive iron with total iron in Black Sea anaerobic/euxinic sediments. Open circles are data from this paper, plus data from Lyons (ms) and Calvert and Karlin (1991). Filled circles are data from Rozanov, Volkov, and Yagodinskaya (1974). Envelopes on highly reactive and poorly reactive iron diagrams define continental margin relationships.
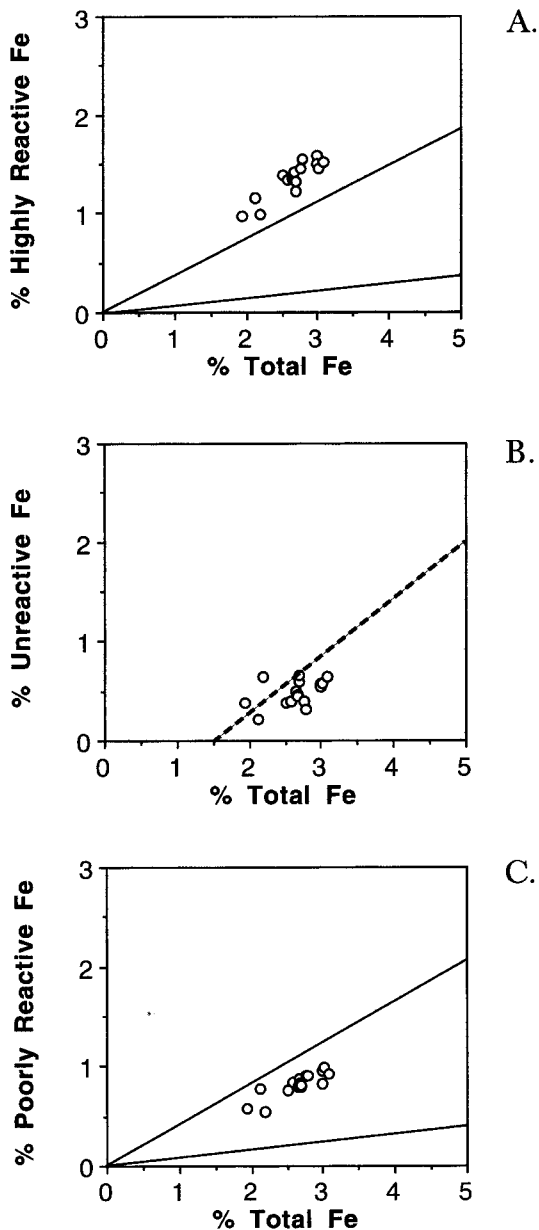
Fig. 6. Variations in the content of (A) highly reactive, (B) unreactive, and (C) poorly reactive iron with total iron in Cariaco Basin anaerobic/euxinic sediments. Envelopes on highly reactive and poorly reactive iron diagrams define continental margin relationships. The dashed line on the unreactive iron diagram defines the relationship seen in the Black Sea sediments (see fig. 5).

The remaining anaerobic/euxinic data from Kau Bay, Orca Basin, and Framvaren show rather variable behavior for Fe_{HR} versus FeT but mainly plot in the field occupied by the aerobic samples, that is below the line defined by eq (1) (fig. 7). The plots of Fe_U and Fe_{PR} for these samples (fig. 7) are rather scattered but, except for some Framvaren
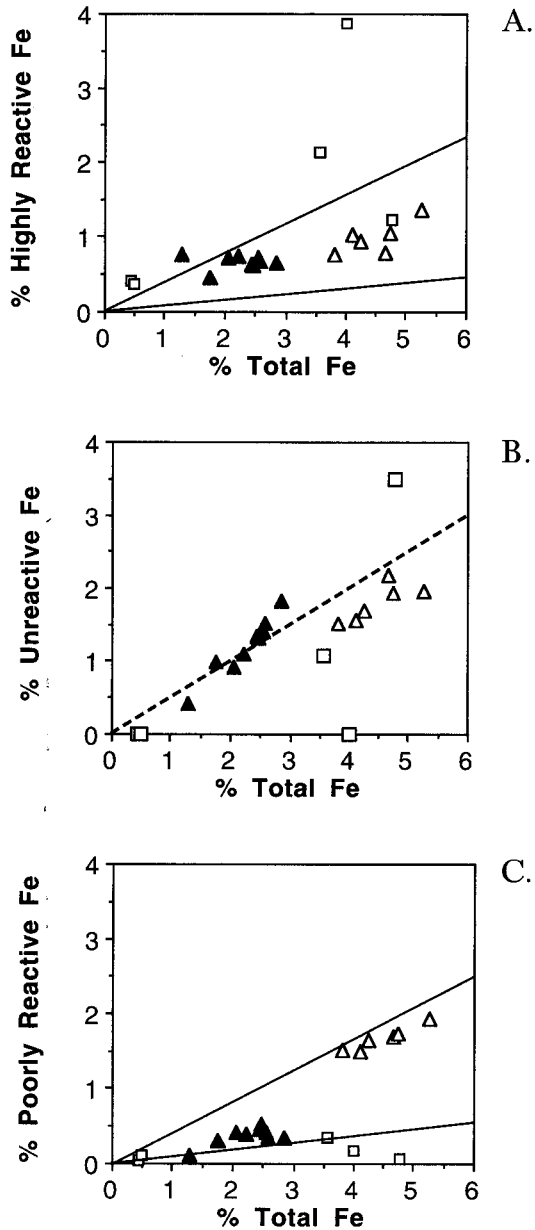
Fig. 7. Variations in the content of (A) highly reactive, (B) unreactive, and (C) poorly reactive iron with total iron in anaerobic/euxinic sediments from Orca Basin (filled triangles), Kau Bay (open triangles), and Framvaren (open squares). Envelopes on highly reactive and poorly reactive iron diagrams define continental margin relationships. The dashed line on the unreactive iron diagram defines the relationship seen in the combined data set of figure 3.

data, are little different to those of the aerobic data set (compare with figs. 3 and 4). Clearly the existence of an anaerobic/euxinic water column is not by itself a sufficient requirement for highly reactive iron enrichment to occur, and further discussion of this issue is given below.

DISCUSSION

Iron speciation in aerobic and dysaerobic sediment.–The aerobic data sets from both continental margin and the deep-sea combined with data from dysaerobic environments demonstrate a strong coherence with respect to Fe speciation. In general, the ranges of behavior with respect to Fe_{HR}, Fe_{PR}, and Fe_U are quite similar. Thus, there is no evidence for particularly large highly reactive Fe contents in deep-sea sediments, as might have been expected with a substantial hydrothermal source of Fe (Chester, 1990). Hence, the sedimentological characteristics that distinguish deep-sea from near-shore sediments (a high proportion of fine-grained clastics and/or biogenous material deposited at low sedimentation rates; Chester, 1990) cannot by themselves produce any significant enrichments in highly reactive iron. Further, as long as some bottom water oxygen is present, its concentration has no apparent influence on Fe speciation as evidenced by a strong overall similarity between the aerobic and dysaerobic data. This has never before been demonstrated but may have been expected given the rapid biological oxidation of reduced iron at seawater pH even under low oxygen conditions (Stumm and Morgan, 1981), and thus the tendancy for Fe to remain within aerobic and dysaerobic sediments, rather than be mobilized from them (Balzer, 1982). This is by contrast with Mn which may be actively mobilized from sediments under low oxygen conditions and high sediment metabolic rates (Sundby, Silverberg, and Chesselet, 1981; Balzer, 1982).

Despite a general similarity between iron speciation for aerobic and dysaerobic samples, there is some geographic variability in the Fe speciation results. In particular, sediments from the northwestern Mediterranean have a rather large amount of highly reactive Fe compared to total Fe, with values of Fe_{HR}/FeT generally above 0.3, exceeding the average for continental margin and deep-sea sediments (table 2). These high ratios may reflect sediments derived from particularly vigorous weathering environments as demonstrated by Canfield (1997) for riverine suspended sediments from the continental United States. In a few cases, relatively high ratios of Fe_{HR}/FeT are observed in deep-sea sediments which could reflect a similar highly weathered terrestrial particle source or a contribution from hydrothermally-derived dissolved Fe at mid ocean ridges.

Iron speciation in anaerobic/euxinic environments.–By contrast with aerobic and dysaerobic environments Fe_{HR} can be enriched in some anaerobic/euxinic sediments. Canfield, Lyons, and Raiswell (1996) have shown that the extent to which sediments are enriched in reactive Fe in the Black Sea is directly correlated with the calcium carbonate content of the sediments. This is because the decaying organic matter that creates the locally high rates of water-column sulfate reduction conducive for iron sulfide precipitation is derived from coccolithophorides. Thus dissolved Fe from the water column is sulfidized and converted to Fe_{HR}, which is intimately associated with the calcareous skeletons of the coccolithophorides. A high correlation between Fe_{HR} and the content of biogenous particles in the sediments ($CaCO_3$) results. Further, the deposition of $CaCO_3$ dilutes the amount of relatively Fe_{HR}-poor lithogenous particles that deposit, enhancing the positive correlation between Fe_{HR} and $CaCO_3$. With no deposition of lithogenous particles this mechanism would produce a sediment composed solely of calcium carbonate and iron sulfides (with some organic matter). By contrast, with no $CaCO_3$ or other biogenous debris, only lithogenous particles would mix with the sulfidized Fe depositing from the water column. Reactive Fe in this case would be mixed with high concentrations of poorly reactive and unreactive Fe as in aerobic and dysaerobic sediments.

One possible mechanism, then, for achieving high proportions of reactive iron is to deposit high concentrations of biogenous material. As stated above, this will dilute the Fe_{PR} and Fe_U contribution of lithogenous particles and enhance the deposition of Fe_{HR} which, according to the model of Canfield, Lyons, and Raiswell (1996), is itself derived indirectly from the decomposition of the organic carbon associated with the inorganic

biogenous particles. This model is extended and applied in figure 8 to all the anaerobic/euxinic data from the present study.

It is apparent that most of the remaining modern anaerobic/euxinic environments (Orca Basin, Cariaco Basin, and Kau Bay, but not Framvaren) plot along the same mixing trend as the euxinic Black Sea sediment. Hence sediments with a higher biogenous component tend also to have a higher ratio of Fe_{HR}/FeT, consistent with the above discussion. The values of the boundary given by eq (1) ($Fe_{HR}/FeT = 0.38$) are also plotted on figure 8, clearly showing that only Cariaco Basin and some Black Sea sediments contain proportionately more Fe_{HR} than aerobic continental margin sediments. These results help us to rationalize the differences observed between the Fe_{HR} contents of these different euxinic sites (figs. 5, 6, and 7). Thus, the elevated reactive iron contents of the Black Sea and Cariaco Basin result from relatively large dilutions of lithogenous particles with biogenous material associated with sulfidized Fe as described above. The other anaerobic/euxinic sites have a lower proportion of biogenous particles and are hence dominated by lithogenous particles with their associated poorly reactive and unreactive components. Other factors such as thickness of the dissolved Fe^{2+}-rich zone could also contribute to the basinal differences observed here. Hence, both the Cariaco Basin and the Black Sea are the deepest basins, with the thickest zones of waters enriched with Fe^{2+}. These basins, then, provide the most amount of time for water-column iron sulfides to form, potentially increasing the amount of sulfidized iron (FeP, which contributes to Fe_{HR}) depositing with the biogenous particles. The trends in figure 8 encourage us to suggest that enrichments in highly reactive iron at high $CaCO_3$ content
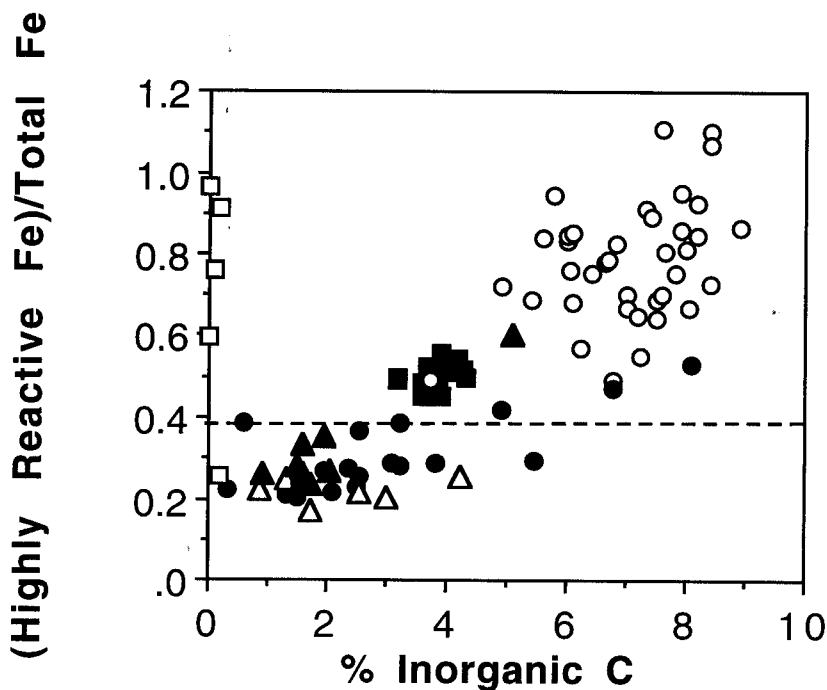
Fig. 8. Variations in the ratio of highly reactive iron to total iron with inorganic C content for anaerobic/euxinic sediments from the Black Sea (open circles for data presented here; filled circles for data from Rozanov, Volkov, and Yagodinskaya, 1974), Cariaco Basin (filled squares), Orca Basin (filled triangles), Kay Bay (open triangles), and Framvaren (open squares). Dashed line indicates the value of the ratio defined by the upper boundary for continental margin sediments (see fig. 2).

may provide a way of recognizing the existence of anaerobic/euxinic water columns in the ancient record. There may, however, be a few caveats.

First, the sediments in the Cariaco Basin contain up to 30 percent opal from diatoms (Lyons, personal communication), and adjustment of the data in figure 8 to account for silica plus carbonate contents would move the Cariaco Basin points to the right although still lying within the same general trend of all the anaerobic/euxinic data. This suggests that the mechanisms of reactive iron enrichment observed in the Black Sea through coccolithophoroid sedimentation may also occur with diatoms and coccolithophoroids in the Cariaco Basin, but this will need further work to establish.

Also, the Framvaren data are quite different from the other anaerobic/euxinic sites, plotting on the vertical axis of figure 8 with high ratios of Fe_{HR}/FeT. These sediments have exceedingly high organic C contents (15 percent or more, see also Taylor, Aplin, and Farrimond, 1996) but low carbonate contents. Clearly the same Fe enrichment mechanism as above can occur, with the sinking organic matter becoming sulfidized in the iron-bearing part of the water column, but iron enrichment will not here be associated with increasing inorganic C.

Mineralogical influences on degree of pyritization.–The abundances of the different iron fractions provide an opportunity to evaluate DOP values in different depositional environments and to make a comparison with the analogous variations in ancient sediments (Raiswell and others, 1988). Such a comparison is not straightforward for two reasons. Firstly, our modern sediment data have been affected by oxidation during storage (which converts pyrite Fe to iron oxides soluble in dithionite and HCl). Oxidation will therefore decrease DOP, measured as FeP/(FeH + FeP). Secondly, some of the modern sediments may have had less time for Fe_{HR} to react with dissolved sulfide compared to their ancient counterparts. Thus, many of the modern sediment samples reported here are near surface samples experiencing only the earliest stages of diagenesis, and few of the cores were deep enough to retrieve sediments with complete sulfate and sulfide consumption. Thus, the later diagenetic addition of pyrite through reaction of pore water sulfide with highly reactive iron is not included, although this addition may not be large (see later).

The combined effects of oxidation and continued reaction of Fe_{HR} can be evaluated by estimating a potential DOP as (FeD + FeP)/(FeP + FeH), which represents the DOP reached if all dithionite-soluble iron were pyritized. Unfortunately FeD also includes small amounts of iron extracted from silicates (Raiswell, Canfield, and Berner, 1994) in addition to that extracted from oxides, hence potential DOP values can only be realized where dithionite-soluble silicate iron has the opportunity to react with dissolved sulfide. Thus samples affected by oxidation (or which have non-sulfidized, dithionite-soluble silicate iron) would have DOP values lying between their measured DOP values and their potential DOP values.

DOP and potential DOP values are plotted in figure 9 for the aerobic continental margin samples and range from 0 to 0.4 and 0.2 to 1.0 respectively. Equivalent ancient sediments have DOP ranging from 0.1 to 0.4 (Raiswell and others, 1988), which are within the range of the modern sediment DOP values but toward the lower end of the potential DOP values. These values indicate that modern sediment DOP values may be somewhat low, probably because of oxidation effects. However potential DOP values appear high by comparison to the ancient sediments. Thus some iron extractable by dithionite does not apparently react with sulfide even under the prolonged diagenetic timescales represented by ancient lithified sediment. Unreacted Fe_{HR} could represent either iron oxides (where insufficient sulfide was present) or dithionite-extractable iron silicates. The amount of such iron has been found to be about 0.1 to 0.2 percent in modern sediments (Canfield, Raiswell, and Bottrell, 1992).
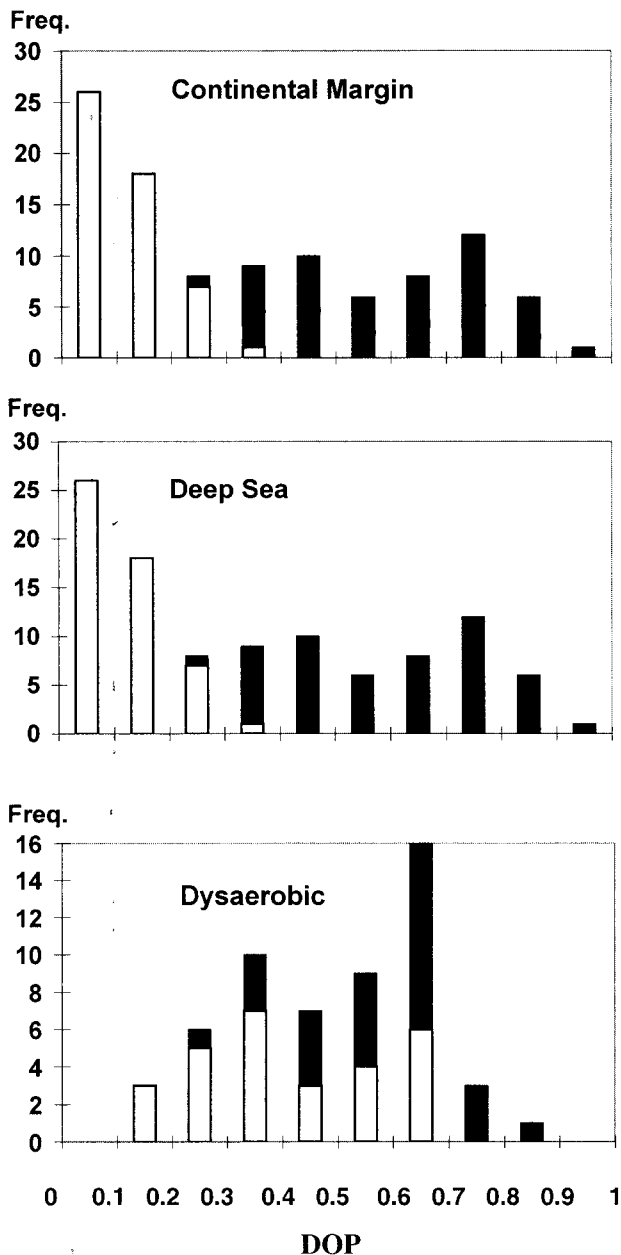
Fig. 9. Frequency of DOP (clear) and potential DOP (infilled) values for continental margin, deep-sea, and dysaerobic sediments.

These conclusions·are reinforced by the DOP (0–0.4) and potential DOP (0.2–1.0) values of the aerobic deep-sea sediments (fig. 9). Again DOP values of the modern sediments are consistent with those of other ancient aerobic samples (0.1–0.4), but potential DOP values are clearly higher. However the deep-sea data contain a high

proportion of sediments from the northwestern Mediterranean, which contain above average proportions of Fe_{HR} (see earlier), and will therefore produce high potential DOP values. The low organic C contents of the deep-sea sediments and consequently their limited capacity for sulfide generation (Canfield, 1991) make it most unlikely that potential DOP values would be realized, and pyrite formation is clearly organic C limited.

The dysaerobic data have DOP values of 0.1 to 0.7 and potential DOP values of 0.2 to 0.9 (fig. 9), whereas equivalent ancient sediments range from 0.5 to 0.8. The potential DOP values here appear more consistent with the range observed in ancient sediments in that fewer samples occur below the minimum DOP values found in the ancient. This perhaps indicates that the more sulfidic dysaerobic sediments are now able to pyritize more, and in most cases nearly all, FeD including the silicate iron extractable by dithionite. This argument is supported by comparing Fe_{HR} values with those in the continental margin samples (see fig. 2), which show that both suites of samples contain essentially the same proportions of highly reactive iron (see earlier). The FeH contents of the two groups of samples are also similar (continental margin 1.32 ± 0.36 percent, dysaerobic 1.43 ± 0.71 percent), so that the higher DOP values of the dysaerobic data set are clearly due to higher pyrite contents (and not lower FeH contents). Note that the sedimentation rates of both groups seem comparable, with most rates falling in the range 0.1 to 1.0 cm yr^{-1} (see app. 1 and 3).

The continental margin, deep-sea, and dysaerobic data are all consistent in indicating that pyritization occurs principally at the expense of iron oxides. Sediment composition apparently does not affect DOP values, because all three depositional environments are similar in Fe_{HR} contents (table 2), and their mean potential DOP values (continental margin 0.55 ± 0.12; deep sea 0.49 ± 0.19; and dysaerobic 0.48 ± 0.14; no significant differences on a student's t test). Hence differences in the DOP values between the three groups of samples must arise because of increasing capacity for sulfide production and reaction in passing from the deep sea to the continental margin and dysaerobic sediments.

The anaerobic/euxinic samples (fig. 10) show a quite considerable variation. DOP in the Black Sea samples ranges from 0.3 to 1.0 with the samples of Rozanov, Volkov, and Yagodinskaya (1974) lying mainly at the lower end of this range. This range in DOP is comparable to that found in Framvaren (0.2–0.8; fig. 11). The Cariaco Basin DOP (0.5–0.7; fig. 10) are rather higher than in the Orca Basin (0.2–0.5) and Kau Bay (0.1–0.3) as shown in figures 10 and 11. Taken together, these values extend to a rather lower range than their ancient sediment analogues (0.5–1.0) and significantly lower than the DOP of 0.75 suggested by Raiswell and others (1988) to represent the boundary between dysaerobic and anaerobic/euxinic samples. Potential DOP values in our Black Sea samples are 0.6 to 1.0, compared to 0.3 to 0.7 for the Black Sea samples of Rozanov, Volkov, and Yagodinskaya (1974), 0.5 to 0.9 for the Orca Basin, 0.5 to 0.7 for the Cariaco Basin, 0.3 to 0.5 for Kau Bay, and 0.7 to 1.0 for Framvaren. Overall the potential DOP data are consistent with the ranges found in their ancient analogues, excepting for the lowest values, which are attributable to the presence of high concentrations of lithogenous debris which dilute the highly reactive iron content (fig. 12).

Clearly the modern sediment DOP values show variations between the aerobic, dysaerobic, and anaerobic/euxinic samples which are similar to or lower than their ancient sediment equivalents. However most of the modern sediments explored here would enter the geologic record with higher DOP values than measured, owing to our inability to collect samples, under most circumstances, where diagenesis is complete. We would anticipate that most sediments of the present study would be preserved with DOP values somewhere between the actual measured DOP's and the potential DOP values.
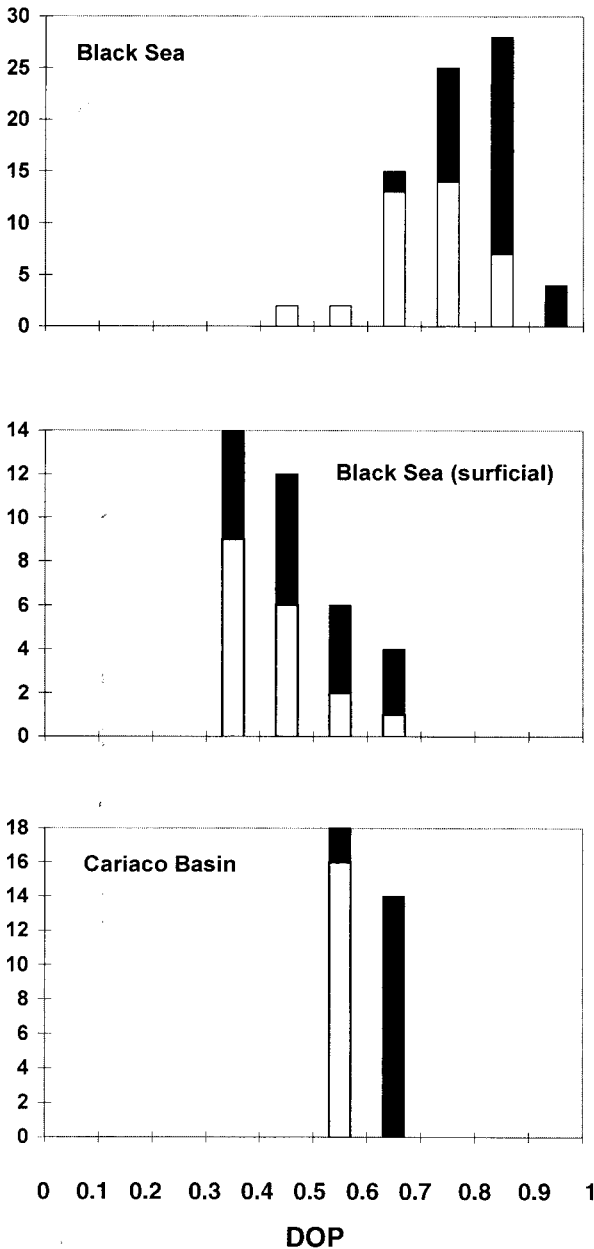
Fig. 10. Frequency of DOP (clear) and potential DOP (infilled) values in Black Sea sediments (surficial data from Rozanov, Volkov, and Yagodinskaya, 1974) and Cariaco Basin sediments.

These results apparently suggest that anaerobic/euxinic samples in the geological record may not always reach DOP values 0.75, as suggested by Raiswell and others (1988). However, excepting the surficial (deep basin but probably turbiditic) Black Sea samples, the potential DOP values below 0.75 were found mainly in small basins located close to land and with relatively high sedimentation rates. Such basins require relatively high biogenous fluxes in order to achieve highly reactive iron contents sufficient to
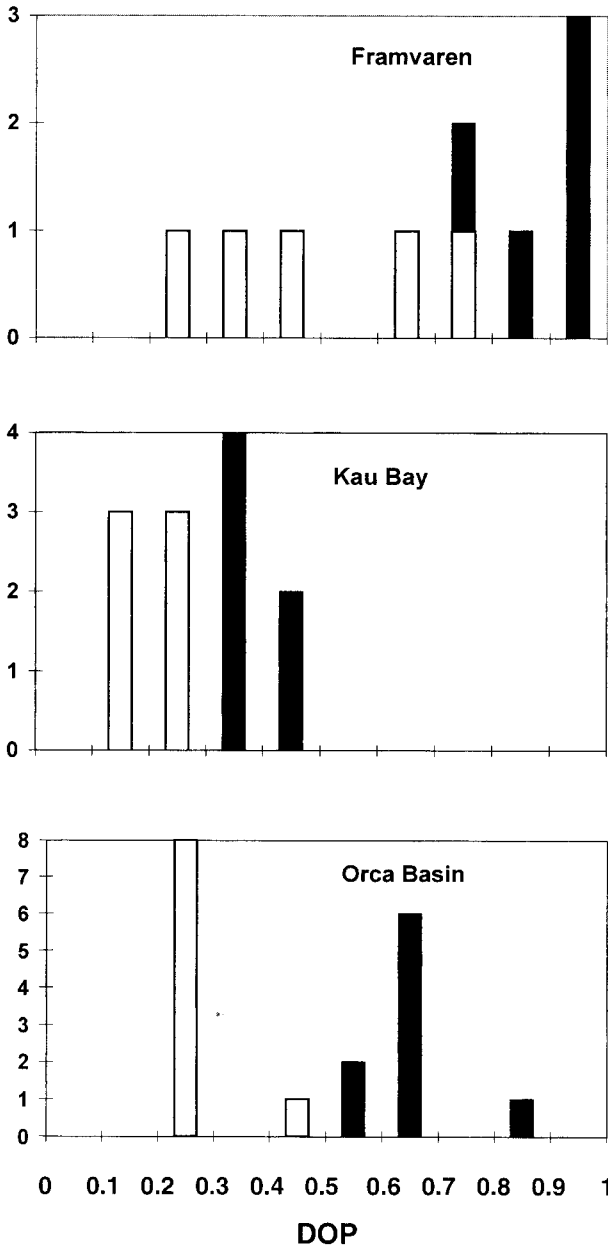
Fig. 11. Frequency of DOP (clear) and potential DOP (infilled) values from Framvaren, Kau Bay, and the Orca Basin sediments.

produce DOP > 0.75. High enough biogenous fluxes are apparently reached in Framvaren, occasionally in the Orca Basin, but not at all in Kau Bay. By contrast, larger basins with substantial areas of deep water remote from land (and thus with low sedimentation rates) will reach a DOP of 0.75 with much lower, more typical biogenous fluxes. Such basins are more likely to predominate in studies of the ancient record by virtue of their size and economic interest.

Fig. 12. Variations in potential DOP values with inorganic C content for anaerobic/euxinic sediments from the Black Sea (open circles for data presented here; filled circles for data from Rozanov, Volkov and Yagodinskaya, 1974), Cariaco Basin (filled squares), Orca Basin (filled triangles), Kay Bay (open triangles), and Framvaren (open squares).

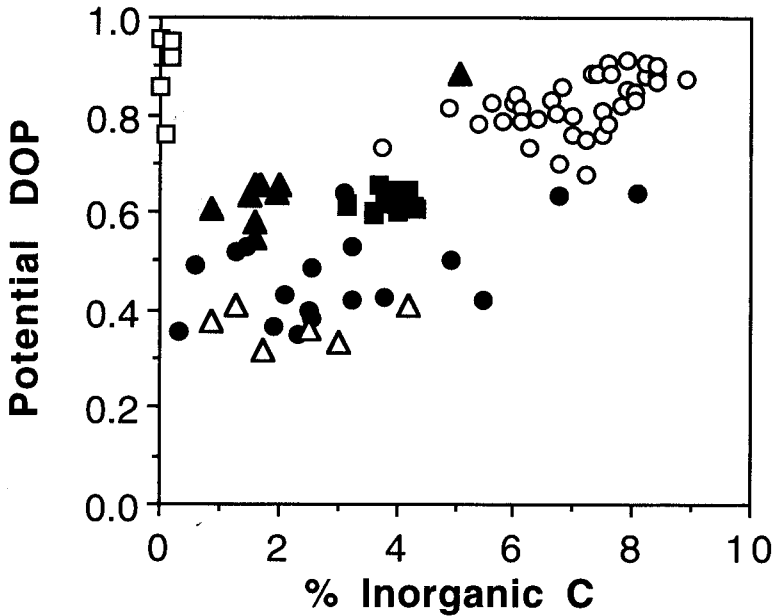## CONCLUSIONS

1. Modern sediments from different depositional environments have been examined for their variations in highly reactive, poorly reactive, and unreactive iron (which together make up the total iron fraction). The proportions of the total iron pool which make up each fraction show very little variation between aerobic continental margin (<1000 m depth), and deep sea (>1000 m depth) sediments and sediments deposited under dysaerobic water conditions. On average the total iron is 25 to 28 percent highly reactive, 23–31 percent poorly reactive and 42–41 percent unreactive.

2. Modern anaerobic/euxinic sediments from the Black Sea (excepting surficial, deep basin samples of possible turbiditic origin), Cariaco Basin, and Framvaren contain a total iron pool enriched in highly reactive iron and depleted in unreactive iron. However Kau Bay, the Orca Basin, and surficial Black Sea sediments contain similar proportions of the different iron fractions as are found in aerobic and dysaerobic environments. The highly reactive iron fraction varies continuously in all these anaerobic/euxinic sediments as a function of the inorganic C content (which indicates a high contribution of biogenous material to the sediment). These data support the model of Canfield, Lyons, and Raiswell (1996), where organic matter associated with the biogenous flux generates pyrite in the water column, effectively enriching the highly reactive iron content. However where lithogenous fluxes are high (Kau Bay, Orca Basin, surficial Black Sea sediments), the biogenous enrichment is diluted, and the sediments assume the characteristics of aerobic and dysaerobic sediments. The enrichments in highly reactive iron provide a way of recognizing the existence of euxinicity in the ancient record, in sediments with approx 50 percent biogenous material.

3. Degrees of pyritization (DOP) values for aerobic and dysaerobic sediments provide a reasonable correspondence with the variations observed in ancient sediments, with different extents of bottom water oxygenation. This indicates that most pyrite is formed by the sulfidation of iron oxides and that the poorly reactive iron fraction is sulfidized only slowly.

4. DOP values for the anaerobic/euxinic sediments are generally lower than their ancient equivalents. The highest DOP values are found in biogenous-rich sediments in the Black Sea (excepting the surficial samples), Cariaco Basin, and Framvaren, but many of these samples have DOP values less 0.75 (whereas their ancient sediment equivalents generally exceed 0.75). Potential DOP values provide a better match to the ancient data, which suggests that dithionite-soluble silicate iron may be sulfidized in these environments.

APPENDIX 1

Description of aerobic (Continental Margin) sediments

Location	Water Depth (m)	Sample Depth (cm)	Sedimentation rate cm yr^{-1}	Reference Number
FOAM, Long Island Sound	9	0–2, 250–260	0.1	1, 2
NWC, Long Island Sound	1.5	0–2, 90–100	0.07	2, 3
Sachem, Long Island Sound	2	6–9, 100–110	1.5	2, 3
K1, Kattegat, Denmark	46	0–0.5, 20–24	0.2	4, 5
K3, Kattegat, Denmark	. 56	0–0.5, 24–28	0.2	4, 5
S1, Skagerrak, Denmark	50	12–13	0.1–0.2	6
S6, Skagerrak, Denmark	380	0–0.5, 24–28	0.1–0.2	6
S7, Skagerrak, Denmark	500	0–2	0.1–0.2	6
Station 18, Mississippi Delta	10	0–3, 30–35	2.0	1, 2
Station 19, Mississippi Delta	75	0–3, 20–30	1.0	1, 2
Station 20, Mississippi Delta	40	40–50, 400–410	0.1–0.2	1, 4, 7
Station 22, Mississippi Delta	100	30–35, 310–320	0.4	1, 4, 7
Station 1, NW Mediterrean, France	100	0–1, 10–12	0.40	8, 9
Station 2, NW Mediterrean, France	44	0–1, 10–12	?	8, 9
Station 4, NW Mediterrean, France	101	0–1, 10–12	0.20	8, 9
Station 5, NW Mediterrean, Spain	760	0–1, 10–12	0.09	8, 9
Station 6, NW Mediterrean, France	85	0–1, 10–12	0.13	8, 9
Station 7, NW Mediterrean, Spain	11	0–1, 10–12	?	8, 9
Station 8, NW Mediterrean, Spain	520	0–1, 10–12	0.15	8, 9
Station 9, NW Mediterrean, Spain	75	0–1, 10–12	0.20	8, 9
Station 11, NW Mediterrean, Spain	30	0–1, 10–12	?	8, 9
Station 13, NW Mediterrean, Spain	27	0–1, 10–12	?	8, 9
Station 16, NW Mediterrean, France	210	0–1, 10–12	0.12	8, 9
Station 17, NW Mediterrean, France	105	0–1, 10–12	?	8, 9

Footnote to column 5 (reference number):
(1) Canfield (1988); (2) Canfield (1989); (3) Canfield and Berner (1987); (4) Canfield (unpublished data); (5) Van Weering (personal communication); (6) Canfield, Thamdrup, and Hansen (1993); (7) Shokes (ms); (8) Blackburn (1992); (9) Zuo, Eisma, and Gieles (1992).

Description of aerobic (deep sea) samples

Location	Water Depth (m)	Sample Depth (cm)	Sediment rate cm yr[1]	Reference number
Station 1, Dakar Transect, Senegal	1332	0.5–1, 4–5	?	1, 2
Station 2, Dakar Transect, Senegal	3799	0–1, 4–5	?	1, 2
Station 3, Dakar Transect, Senegal	2981	1–2, 3–4	?	1, 2
Domes Site A, North Pacific 9°2′N, 151°11′W	5040	6–7	1.5×10^{-4}	3
Domes Site B, North Pacific 11°15′N, 139°4′W	4831	9–10	3.0×10^{-4}	3
Domes Site C, North Pacific 15°10′N, 125°54′W	4638	11–13	1.4×10^{-4}	3
VM 26 103, South Atlantic 0°29′S, 39°32′W	4001	54–56	?	4
VM 27 265, North Atlantic 36°6′N, 43°41′W	4945	44–46	?	4
VM 28 98, North Atlantic 26°47′N, 50°50′W	4083	45–46	?	4
VM 28 90, North Atlantic 42°10′N, 42°6′W	4863	33–35	?	4
VW 28 101, North Atlantic 30°30′N, 54°15′W	5592	41–44	?	4
VM 28 207, Pacific 2°0′N, 175°0′W	5000	43–47	?	4
VW 30 021, Atlantic 6°35′N, 42°47′W	4490	6–7, 54–57	?	4
VM 30 089, North Atlantic 36°22′N, 41°57′W	4256	24–28, 51–54	?	4
VM 31 152, North Atlantic 23°47′N, 45°46′W	4174	52–56	?	4
VM 32 64, North Atlantic 20°40′N, 32°13′W	4900	42–47	?	4
VM 32 71, North Atlantic 10°27′N, 44°40′W	4947	34–37	?	4
RC 13 54, North Pacific 14°0′N, 173°0′W	5000	35–40	?	4
RC 20 07, North Pacific, 5°58′N, 147°19′W	4988	40–50	?	4
VM 31 157, North Atlantic, 26°N, 45°25′W	3343	45–47	?	4
VM 32 154, North Pacific, 41°49′N, 133°15′W	3482	8–9, 54–58	?	4
VM 32 173, South Pacific 4°16′S, 168°52′E.	3261	52–57	?	4
Station N, California	4078	11–12, 39–40	?	5, 6
Station M, California	3730	5–6, 29–30	0.02	5, 6
Station G, California	3340	21–22, 23–24	0.005–0.08	5, 6
Station 20, Eastern Mediterrean	2412	0.5, 8	0.003	7
Station 22, Eastern Mediterrean	2883	0.5, 5	0.003	7
Station 23, Eastern Mediterrean	1907	0.5, 5	0.003	7
Station UH 35, Eastern Mediterrean	2672	0.5, 5.5	0.003	7
Station 3, Northwest Mediterrean, Spain	1670	0–1, 10–12	0.04	8, 9
Station 10, Northwest Mediterrean, Spain	1080	0–1, 10–12	0.07	8, 9
Station 12, Northwest Mediterrean, Spain	1790	0–1, 10–12	0.05	8, 9
Station 14, Northwest Mediterrean, Spain	2390	0–1, 10–12	0.03	8, 9
Station 15, Northwest Mediterrean, Spain	2500	0–1, 10–12	0.025	8, 9
C-40, Chile, 36°20′S, 73°44′W	1015	0–0.5, 8–10	0.05–0.1	10
C-41, Chile, 36°20′S, 73°49′W	2000	0–0.5, 8–10	0.05	10

Footnote to column 5 (reference number):
(1) Jahnke and others (1989); (2) Ruttenberg (personal communication); (3) Cochran and Krishnaswami (1980); (4) Lamont-Doherty Core Catalogue; (5) Reimers and others (1992); (6) Ingall (personal communication); (7) Strohle (ms); (8) Blackburn (1992); (9) Zuo, Eisma, and Geiles (1992); (10) Salamanca (personal communication).

Description of dysaerobic samples

Location	Water Depth (m)	Sample Depth (cm)	Sediment rate cm yr^{-1}	Reference Number
Santa Barbara, Basin	590	1, 5	0.4	1
Gulf of California, L121	697	5–11, 52–57	0.2	2
Gulf of California, L139	410	16–33, 247–254	0.2	2
Gulf of California, L62	260	5–10, 38–46	0.2	2
Gulf of California, L42	602	29–38, 45–50	0.2	2
Gulf of California, L154	496	35–42, 54–61	0.2	2
Gulf of California, L105	?	8–14, 84–90	0.2	2
Station D, California, Shelf	1443	5–6, 29–30	0.0013	3, 4
Station J, California, Shelf	781	15–16, 39–40	0.013	3, 4
Station K, California, Shelf	998	11–12, 29–30	0.008	3, 4
Chile, C6, 36°37′S, 73°00′W	34	8	0.1–0.2	5
Chile, C7, 36°36′S, 73°00′W	37	8	0.1–0.2	5
Chile, C18, 36°30′S, 73°07′W	87	1, 8	0.17	5
Chile, C26, 36°25′S, 73°23′W	122	1, 8	0.1–0.2	5

Footnote to column 5 (reference number):
(1) Sholkolovitz (1973); (2) Berner (1964); (3) Reimers and others (1992); (4) Ingall (personal communication); (5) Salamanca (personal communication).

APPENDIX 4

Description of anaerobic/euxinic samples

Location	Water Depth (m)	Sample Depth (cm)	Sediment Rate cm yr^{-1}	Reference Number
Orca Basin	2000	1, 5, 6, 7, 8, 9, 10, 11, 12	0.1	1, 2
Station 9, Black Sea	2094	6–8, 8–10, 12–14, 14–16, 20–22, 24–26	0.02	3, 4
Station 14, Black Sea	2218	10–12, 20–22	0.02	3, 4
Station 9, Black Sea	2094	3, 5, 7, 9, 11, 13, 15, 17, 19, 21, 23, 25	0.02	5
Station 14, Black Sea	2218	7, 9, 11, 13, 15, 17, 19, 21, 23, 25, 27, 29	0.02	5
Station 14, Black Sea	2218	Surface, 5–10, 10–15, 15–20, 20–25	0.02	3, 4
Deep Basin Sediments, (>500m), Black Sea				
Station 286	473	Surface	0.02	6
Station 245	630	Surface	0.02	6
Station 223	640	Surface	0.02	6
Station 287	795	Surface	0.02	6
Station 257	640	Surface	0.02	6
Station 9	964	Surface	0.02	6
Station 223	700	Surface	0.02	6
Station 235	1800	Surface	0.02	6
Station 288	1320	Surface	0.02	6
Station 278	1215	Surface	0.02	6
Station 256	1340	Surface	0.02	6
Station 214	1620	Surface	0.02	6
Station 243	2125	Surface	0.02	6
Station 4751	2222	Surface	0.02	6
Station 289	2016	Surface	0.02	6
Station 4740	2012	Surface	0.02	6
Station 255	2060	Surface	0.02	6
Station 254	2200	Surface	0.02	6
K3, Kau Bay, Indonesia	457	2–3	0.07	7
K4-85077, Kau Bay, Indonesia	414	6–7	0.07	7
K4-85471, Kau Bay, Indonesia	440	3–4	0.07	7
K9, Kau Bay, Indonesia	410	2–4	1.0	7
K11-85475, Kau Bay, Indonesia	260	7–8	0.085	7
K11-85476, Kau Bay, Indonesia	260	44–45	0.085	7
Framvaren	45	0–2, 2–4	0.01	8, 9
Framvaren	177–185	Surface, 0–2	0.01	8, 9
Cariaco Trench, Site 1002B				
Core B1	500	15–20, 35–40, 55–60, 65–70, 125–130, 145–150	0.06	10, 11
Core B2	500	20–25, 65–70, 125–130, 140–145	0.06	10, 11
Core B3	500	20–25, 60–65, 145–150	0.06	10, 11
Core B4	500	20–25, 60–65, 80–85	0.06	10, 11

Footnote to column 5 (reference number):
   (1) Bacon and others (1980); (2) Trefry and others (1984); (3) Lyons (1992); (4) Lyons and Berner (1992); (5) Calvert and Karlin (1991); (6) Rozanov, Volkov, and Yagodinskaya (1974); (7) Middelburg (ms and 1991); (8) Skei (1983); (9) Saelen and others (1993); (10) Scranton and others (1987); (11) Lyons and others (1996).

REFERENCES

Aller, R. C., Mackin, J. E., and Cox, R. T. Jr, 1986, Diagenesis of Fe and S in Amazon inner shelf muds: apparent dominance of Fe reduction and implications for the genesis of ironstones: Continental Shelf Research, v. 6, p. 263–289.
Arthur, M. A., Dean, W. E., Neff, E. D., Hay, B. J., King, J., and Jones, G., 1994, Varve calibrated records of carbonate and organic carbon accumulation over the last 2000 years in the Black Sea: Biogeochemical Cycles, v. 8, p. 195–217.
Bacon, M. P., Brewer, P. G., Spencer, D. W., Murray, J. W., and Goddard, J., 1980, Lead-210, polonium-210, manganese and iron in the Cariaco Trench: Deep Sea Research, v. 27A, p. 119–135.
Balzer, W., 1982, On the distribution of iron and manganese at the sediment/water interface: thermodynamic versus kinetic control: Geochimica et Cosmochimica Acta, v. 46, p. 1153–1161.

Berner, R. A., 1964, Distribution and diagenesis of sulfur in some sediments from the Gulf of California: Marine Geology, v. 1, p. 117–140.
———— 1970, Sedimentary pyrite formation: American Journal of Science, v. 268, p. 2–23.
———— 1984, Sedimentary pyrite formation: an update: Geochimica et Cosmochimica Acta, v. 48, p. 606–616.
Blackburn, T. H., 1992, Mineralization in North Western Mediterranean Sea: Cybele cruise, in Martin, J. M., and Barth, H., editors, EROS Workshop Third, Brussels, Belgium: Den Burg, Netherlands, Comission of the European Communities, p. 469–479.
Brewer, P. G., and Spencer, D. W., 1974, Distribution of some trace elements in Black Sea and their flux between dissolved and particulate phases, in Degens, E. T., and Ross, D. A., editors, The Black Sea-Geology, Chemistry and Biology: Tulsa, Oklahoma, American Association of Petroleum Geologists, p. 137–143.
Calvert, S. E., and Karlin, R. E., 1991, Relationships between sulphur, organic carbon and iron in the modern sediments of the Black Sea: Geochimica et Cosmochimica Acta, v. 55, p. 2483–2490.
Canfield, D. E., ms, 1988, Sulfate reduction and the diagenesis of iron in anoxic marine sediments: Ph.D. dissertation, Yale University, 248p.
———— 1989, Reactive iron in marine sediments: Geochimica et Cosmochimica Acta, v. 53, p. 619–632.
———— 1991, Sulfate reduction in deep-sea sediments: American Journal of Science, v. 291, p. 177–188.
———— 1997, The geochemistry of river particulates from the continental United states: major elements: Geochimica et Cosmochimica Acta, v. 61, p. 3349–3365.
Canfield, D. E., and Berner, R. A., 1987, Dissolution and pyritisation of magnetite in anoxic marine sediments: Geochimica et Cosmochimica Acta, v. 51, p. 645–659.
Canfield, D. E., Lyons, T. W., and Raiswell, R., 1996, A model for iron deposition to euxinic Black Sea sediments: American Journal of Science, v. 296, p. 818–834.
Canfield, D. E., and Raiswell, R., 1991, Pyrite formation and fossil preservation, in Allison, P. A., and Briggs, D. E. G., editors, Topics in Geobiology: New York, Plenum Press, p. 337–387.
Canfield, D. E., Raiswell, R., and Bottrell, S. H., 1992, The reactivity of sedimentary iron minerals towards sulfide: American Journal of Science, v. 292, p. 659–683.
Canfield, D. E., Raiswell, R., Westrich, J. T., Reaves, C. M., and Berner, R. A., 1986, The use of chromium reduction in the analysis of reduced sulfur in sediments and shales: Chemical Geology, v. 54, p. 149–155.
Canfield, D. E., Thamdrup, B., and Hansen, J. W., 1993, The anaerobic degradation of organic matter in Danish coastal sediments: iron reduction, manganese reduction and sulfate reduction: Geochimica et Cosmochimica Acta, v. 57, p. 3867–3883.
Chester, R., 1990, Marine Geochemistry: London, England, Unwin Hyman, 698 p.
Cochran, J. K., and Krishnaswami, S., 1980, Radium, thorium, uranium and ^{210}Pb in deep-sea sediments and sediment pore waters from the north equatorial Pacific: American Journal of Science, v. 280, p. 849–889.
Crusius, J., and Anderson, R. F., 1991, Immobility of ^{210}Pb in Black Sea sediments: Geochimica et Cosmochimica Acta, v. 55, p. 327–33.
Goldhaber, M. B., and Kaplan, I. R., 1974, The sulfur cycle, in Goldberg, E. D., editor, The Sea: New York, Wiley Interscience, p. 569–655.
Jahnke, R. A., Emerson, S. R., Reimers, C. E., Schuffert, J., Ruttenberg, K., and Archer, D., 1989, Benthic recycling of biogenic debris in the eastern tropical Atlantic Ocean: Geochimica et Cosmochimica Acta, v. 53, p. 2947–2960.
Leventhal, J. S., and Hosterman, J. W., 1982, Chemical and mineralogical investigations of Devonian Black shale samples from Kentucky, Ohio, West Virginia and Tennessee: Chemical Geology, v. 37, p. 239–264.
Luther, G. W. III, 1991, Pyrite synthesis via polysulfide compounds: Geochimica et Cosmochimica Acta, v. 55, p. 2839–2849.
Lyons, T. W., ms, 1992, Contrasting sediment types from oxic and anoxic sites of the modern Black Sea: Geochemical and sedimentological criteria: Ph.D. dissertation, Yale University, 377 p.
Lyons, T. W., and Berner, R. A., 1992, Carbon-sulfur-iron systematics of the uppermost deep-water sediments of the Black Sea: Chemical Geology, v. 99, p. 1–27.
Lyons, T. W., Pearson, D. G., Murray, R. W., and ODP Leg 165 Scientific Party, 1996, A comparitive study of diagenetic pathways in sediments of the Caribbean Sea and the Cariaco Trench: preliminary results from ODP Leg 165, in Bottrell, S. H., editor, Proceedings of the Fourth International Symposium on the Geochemistry of the Earth's Surface: Leeds, University of Leeds, Department of Earth Sciences, p. 160–163.
Middelburg, J. J., ms, 1990, Early diagenesis and authigenic mineral formation in anoxic sediments of Kau Bay, Indonesia: Ph.D. dissertation, Utrecht University, 176p.
———— 1991, Organic carbon, sulphur, and iron in recent semi-euxinic sediments of Kau Bay, Indonesia: Geochimica et Cosmochimica Acta, v. 55, p. 815–828.
Morse, J. W., and Berner, R. A., 1995, What determines sedimentary C/S ratios?: Geochimica et Cosmochimica Acta, v. 59, p. 1073–1077.
Morse, J. W., and Wang, Q., 1997, Pyrite formation under conditions approximating to those in anoxic sediments: II. Influence of precursor iron minerals and organic matter: Marine Chemistry, v. 57, p. 187–193.
Newton, R., Bottrell, S. H., Dean, S. P., Hatfield, D., and Raiswell, R., 1995, An evaluation of the use of the chromous chloride reduction method for the isotopic analysis of pyrite in rocks and sediments: Chemical Geology, v. 125, p. 317–320.
Raiswell, R., Buckley, F., Berner, R. A., and Anderson, T. F., 1988, Degree of pyritization of iron as a paleoenvironmental indicator: Journal of Sedimentary Petrology, v. 58, p. 812–819.
Raiswell, R., and Canfield, D. E., 1996, Rates of reaction between silicate iron and dissolved sulfide in Peru Margin sediments: Geochimica et Cosmochimica Acta, v. 60, p. 2777–2787.

Raiswell, R., Canfield, D. E., and Berner, R. A., 1994, A comparison of iron extraction methods for the determination of degree of pyritisation and the recognition if iron-limited pyrite formation: Chemical Geology, v. 111, p. 101–111.

Reimers, C. E., Jahnke, R. A., and McCorkle, D. C., 1992, Carbon fluxes and burial rates over the continental slope and rise off central California with implications for the global carbon cycle: Global Biogeochemical Cycles, v. 6, p. 199–224.

Rhoads, D. C., and Morse, J. W., 1971, Evolutionary and ecological significance of oxygen-deficient marine basins: Lethaia, v. 4, p. 413–428.

Rhoads, D. C., Mulslow, S. G., Gutschik, R., Baldwin, C. T., and Stolz, J. F., 1991, The dysaerobic zone revisited: a magnetic facies?, *in* Tyson, R. V., and Pearson, T. H., editors, Modern and continental shelf anoxia: Geological Society of London Special Publication 58, p. 187–199.

Rickard, D. T., 1975, Kinetics and mechanisms of pyrite formation at low temperatures: American Journal of Science, v. 275, p. 636–652.

—— 1997, Kinetics of pyrite formation by the H_2S oxidation of iron(II) monosulfide in aqueous solutions between 25°C and 125°C: the rate equation: Geochimica et Cosmochimica Acta, v. 61, p. 115–134.

Rickard, D. T., and Luther, G. W. III., 1997, Kinetics of pyrite formation by the H_2S oxidation of iron(II) monosulfide in aqueous solutions between 25°C and 125°C: the mechanism: Geochimica et Cosmochimica Acta, v. 61, p. 135–147.

Rozanov, A. G., Volkov, I. I., and Yagodinskaya, T. A., 1974, Forms of iron in surface layer of Black Sea sediments, *in* Degens, E. T., and Ross, D. A., editors, The Black Sea–Geology, Chemistry and Biology: Tulsa, Oklahoma, American Association Petroleum Geologists, p. 532–541.

Saelen, G., Raiswell, R., Talbot, M. R., Skei, J. M., and Bottrell, S. H., 1993, Heavy sedimentary sulfur isotopes as indicators of super-anoxic bottom-water conditions: Geology, v. 21, p. 1091–1094.

Savrda, C. E., Bottjer, D. J., and Gorsline, D. S., 1984, Development of a comprehensive oxygen-deficient marine biofacies model: evidence from Santa Monica, San Pedro and Santa Barbara Basins, California Continental Borderland: Bulletin American Association of Petroleum Geologists, v. 68, p. 1179–1192.

Schoonen, M. A. A., and Barnes, H. L., 1991, Reactions forming pyrite and marcasite from solution, II. Via FeS precursors below 100°C: Geochimica et Cosmochimica Acta, v. 55, p. 1505–1514.

Scranton, M. I., Sayles, F. L., Bacon, M. P., and Brewer, P. G., 1987, Temporal changes in the hydrography and chemistry of the Cariaco Trench: Deep-Sea Research, v. 34, p. 945–963.

Sheu, Der-Duen and Presley, B. J., 1986, Variations of calcium carbonate, organic carbon and iron sulfides in anoxic sediment from the Orca Basin, Gulf of Mexico: Marine Geology, v. 70, p. 103–118.

Shokes, R. F., ms, 1976, Rate-dependent distribution of lead-210 and interstitial sulfate in sediments of the Mississippi River Delta: Ph.D. dissertation, Texas A and M University, 122 p.

Sholkovitz, E. R., 1973, Interstitial water chemistry of the Santa Barbara Basin sediments: Geochimica et Cosmochimica Acta, v. 37, p. 2043–2073.

Skei, J., 1983, Geochemical and sedimentological considerations of a permantly anoxic fjord-Framvaren, south Norway: Sedimentary Geology, v. 36, p. 131–145.

Strohle, K-D, ms, 1996, Early marine diagenesis in two contrasting sedimentary environments: Ph.D. dissertation, Leeds University, 288p.

Stumm, W., and Morgan, J. J., 1981, Aquatic Chemistry: New York, Wiley-Interscience, 780p.

Sundby, B., Silverbeg, N., and Chesselet, R., 1981, Pathways of manganese in an open estuarine system: Geochimica et Cosmochimica Acta, v. 45, p. 393–307.

Taylor, P. D., Aplin, A. C., and Farrimond, J., 1996, Very rapid (<50 yr) incorporation of sulphur into organic and inorganic phases of Framvaren Fjord sediments, *in* Bottrell, S. H., editor, Proceedings of the Fourth International Symposium on the Geochemistry of the Earth's Surface: Leeds, University of Leeds, Department of Earth Sciences, p. 121–123.

Trefry, J. H., Presley, B. J., Keeney-Kennicutt, W. L., and Trocine, R. P., 1984, Distribution and chemistry of manganese, iron and suspended particulates in Orca Basin: Geo-Marine Letters, v. 4, p. 125–130.

Tyson, R. V., and Pearson, T. H., 1991, Modern and ancient continental shelf anoxia: an overview, *in* Tyson, R. V., and Pearson, T. H., editors, Modern and continental shelf anoxia: Geological Society of London Special Publication 58, p. 1–26.

Wallmann, K., Hennies, K., Konig, I., Petersen, W., and Knauth, H., 1993, New procedure for determining reactive Fe(III) and Fe(II) minerals in sediments: Limnology and Oceanography, v. 38, p. 1803–1812.

Wignall, P. B., 1994, Black Shales: Oxford, Clarendon Press, 127p.

Zuo, Z., Eisma, D., and Gieles, R., 1992, Effect of particle transport and mixing on ^{210}Pb distribution in the Northwest Mediterranean Sea, *in* Martin J. M., and Barth, H., editors, EROS Workshop, Third, Brussels, Belgium: Den Burg, Netherlands, Comission of the European Communities, p. 425–436.